LU TP 94-13
hep-ph/9410244
September 1994

# A Simple Prescription for First Order Corrections to Quark Scattering and Annihilation Processes*

**Michael H. Seymour**†
Department of Theoretical Physics, University of Lund,
Sölvegatan 14A, S-22362 Lund, Sweden

## Abstract

We formulate the first order corrections to processes involving the scattering or annihilation of quarks in a form in which the QCD and electroweak parts are exactly factorised. This allows for a straightforward physical interpretation of effects such as lepton-hadron correlations, and a simpler Monte Carlo treatment.

LU TP 94-13
September 1994

*Work supported in part by the EEC Programme "Human Capital and Mobility", Network "Physics at High Energy Colliders", contract CHRX-CT93-0537 (DG 12 COMA).

†Address after 1st January 1995: CERN TH Division, CH-1211 Geneva 23, Switzerland.

# 1 Introduction

Although the parton model has been very successful in providing a qualitative description of $e^+e^-$ annihilation to hadrons, deep inelastic lepton-hadron scattering (DIS), and Drell-Yan lepton pair production, a more detailed description requires higher-order QCD corrections. These have been known for many years to first order in $\alpha_s$, and more recently to second order, but are generally presented in an inclusive form. However, in many instances, a more exclusive treatment is needed, for example to describe features of the hadronic final state or correlations between the hadronic and leptonic parts of the process. This is particularly true of Monte Carlo event generators, where the aim is to provide a fully exclusive description of the process, event by event.

In this paper we present the first order tree-level corrections to quark scattering and annihilation processes in a form in which the QCD and electroweak parts *exactly* factorise. This makes exclusive event features and correlations particularly transparent. We also discuss how these could be used to provide a simple Monte Carlo treatment of the processes. We essentially follow the method of Ref. [1] for $e^+e^-$ annihilation, taking over most of the same notation.

In anticipation of the main applications of our results, we use the language of the DIS and Drell-Yan processes, but in fact our method is applicable to any electroweak process in which the lowest-order diagrams contain a single quark line attached to a single gauge boson. It should also be stressed that the method treats the quarks as massless throughout.

The paper is set out as follows: In the remainder of this section, we recap the important ingredients of [1]. In section 2 we follow the same method to derive the equivalent expression for the QCD Compton part of the first-order correction to DIS (QCDC, $q\ell \to qg\ell$). In section 3 we do the same for the boson gluon fusion part (BGF, $g\ell \to q\bar{q}\ell$). In section 4 as an example of the simplicity of our form, we discuss lepton-hadron correlations in DIS, which have been proposed as an important test of QCD[2,3]. In section 5 we derive and discuss the equivalent results for the Drell-Yan process. Finally in section 6 we give a summary.

The tree-level Feynman diagrams for $e^+e^-$ annihilation to hadrons at $\mathcal{O}(\alpha_s)$ are shown in Fig. 1. It is well known that only the sum of the two diagrams is gauge invariant, and that they can never be separated. However, the first important step of [1] is to use the explicit gauge choice introduced by the CALKUL collaboration[4], in which the diagrams only contribute to physically distinct processes, with all the interference absorbed into the form of the polarisation tensor. In this gauge, only the first diagram of Fig. 1 contributes to final states in which the gluon has the same helicity as the quark, and the second diagram when it has the same helicity as the antiquark. The polarisation tensor contains collinear-divergent pieces, so that both diagrams still give collinear divergences in both directions.

The next important step is to introduce a pair of massless four-vectors $r_{1,2}$

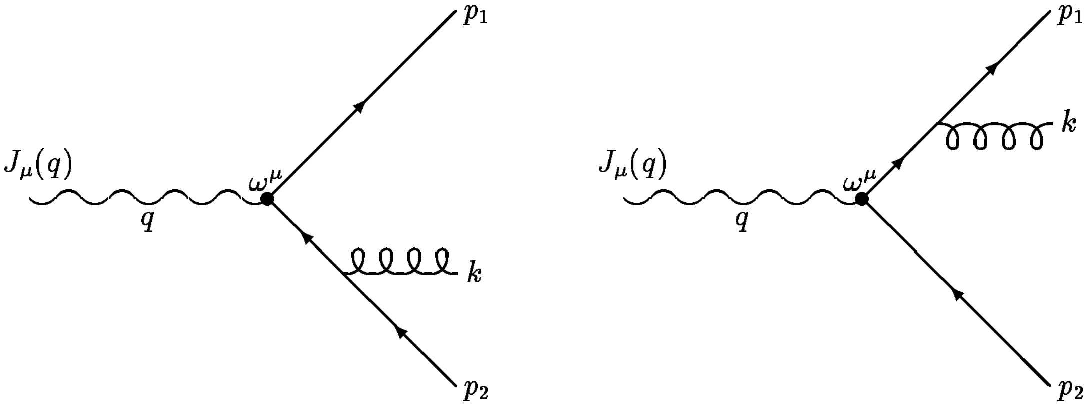


Figure 1: Tree-level Feynman diagrams for $e^+e^- \to$ hadrons at $\mathcal{O}(\alpha_s)$, in which the lepton side is represented by an arbitrary current, $J_\mu$, and the boson-quark coupling by $\omega^\mu$.

that are parallel to $p_{1,2}$ but with energy $Q/2$, the energy of the partons in the parton model. These allow each matrix element to be written as the product of two parts, one corresponding to parton-model production, the other to the emission of the gluon without any knowledge of $J_\mu$ or $\omega^\mu$. The final result is then

$$d\sigma_3 = \frac{C_F \alpha_s}{2\pi} d\Gamma_2 \frac{dx_1 dx_2}{(1-x_1)(1-x_2)} \frac{d\phi}{2\pi} \left\{ x_1^2 |\mathcal{M}_2(r_1, q-r_1)|^2 + x_2^2 |\mathcal{M}_2(q-r_2, r_2)|^2 \right\}, \tag{1}$$

where $x_i \equiv 2\, p_i{\cdot}q \,/\, q{\cdot}q$ are the energy fractions in the cmf of $q$, $d\Gamma_2$ is an element of the parton-model phase-space, and $\phi$ is the azimuthal angle of the gluon. Both $d\Gamma_2$ and $\phi$ have different interpretations for the two parts of the matrix element: in the first they refer to the phase-space to produce a quark with momentum $r_1$ in the parton model, and the azimuthal angle around $r_1$, while in the second they refer to an antiquark with momentum $r_2$. With the exception of neglecting quark masses, this expression is exact for arbitrary currents of vector or axial-vector type, so applies equally well to the W decays in WW pair production for example. It is also valid at the helicity level, so if polarisation effects are retained in the lowest-order matrix element, they are correctly treated at $\mathcal{O}(\alpha_s)$.

As a Monte Carlo prescription, (1) has a simple interpretation: first parton-model events are generated according to the exact matrix element, then gluon emission is generated according to

$$\frac{1}{\sigma_0} \frac{d\sigma}{dx_1 dx_2} = \frac{C_F \alpha_s}{2\pi} \frac{x_1^2 + x_2^2}{(1-x_1)(1-x_2)}, \tag{2}$$

and finally parton 1 or 2 is chosen with relative probability $x_1^2$ and $x_2^2$ to retain its parton-model direction, with the hadron plane being rotated uniformly in azimuth about it. The quarks retain their lowest-order polarisation states, with the gluon inheriting the same state as the parton that was chosen.

This procedure produces the exact distribution of three-parton final states, with no knowledge of the mechanism that produced them, provided an exact generator of two-parton final states is available.

# 2 QCD Compton Process in DIS

## 2.1 The Matrix Element

The three-parton matrix element for a quark of helicity $\lambda$ and a gluon of helicity $\rho$ is given by

$$\mathcal{M}_3(\lambda,\rho) = ig_s\bar{u}_\lambda(p_2)\left[\not\epsilon_\rho(k)\frac{-(\not p_2+\not k)}{2\,p_2\cdot k}\omega^\mu + \omega^\mu\frac{-(\not p_1-\not k)}{-2\,p_1\cdot k}\not\epsilon_\rho(k)\right]u_\lambda(p_1)J_\mu(q), \quad (3)$$

where the momentum of the incoming(outgoing) quark is $p_1(p_2)$, and the gluon is $k$. All the partons are considered massless. We use the explicit formulation of the gluon polarisation tensor $\epsilon_\rho(k)$ introduced by the CALKUL collaboration,

$$\begin{aligned} \not\epsilon_\rho(k) &= N\left(\tfrac{1}{2}(1+\rho\gamma^5)\not k\not p_2\not p_1 - \not p_2\not p_1\not k\tfrac{1}{2}(1+\rho\gamma^5)\right), & (4)\\ N &= [4\,p_1\cdot k\ \ p_2\cdot k\ \ p_1\cdot p_2\,]^{-\frac{1}{2}}. & (5) \end{aligned}$$

After a little manipulation, we obtain

$$\begin{aligned} \mathcal{M}_3^+ \equiv \mathcal{M}_3(\lambda,\ \ \lambda) &= -ig_sN\bar{u}_\lambda(p_2)\omega^\mu(\not p_1-\not k)\not p_2 u_\lambda(p_1)J_\mu(q), & (6)\\ \mathcal{M}_3^- \equiv \mathcal{M}_3(\lambda,-\lambda) &= -ig_sN\bar{u}_\lambda(p_2)\not p_1(\not p_2+\not k)\omega^\mu u_\lambda(p_1)J_\mu(q). & (7) \end{aligned}$$

The special vectors we introduce are defined covariantly by the momentum fractions of the partons,

$$x_i \equiv \frac{2\,p_i\cdot q}{q\cdot q}, \quad (8)$$

just as in $e^+e^-$ annihilation. In general $x_1 \le -1,\ x_2 \le 1$, where the equalities apply in the parton-model scattering case.

$$\begin{aligned} r_1 &\equiv -p_1/x_1, & (9)\\ \bar{r}_2 &\equiv \ \ r_1+q = p_2+k-p_1-p_1/x_1, & (10)\\ r_2 &\equiv \ \ p_2/x_2, & (11)\\ \bar{r}_1 &\equiv \ \ r_2-q = p_1-k-p_2+p_2/x_2. & (12) \end{aligned}$$

It can be seen that $r_1,\bar{r}_2$ are the momenta that the incoming and outgoing quarks would have in $\mathcal{O}(1)$ scattering at the same $y_{\rm B}$ and $Q^2$. $\bar{r}_1, r_2$ have the same component parallel to the current direction, but also have a component transverse to it, such that $r_2$ is parallel to $p_2$. As we discuss in more detail later, these are the momenta that the incoming and outgoing quarks would have in the parton model with an 'intrinsic' $p_t$.

We can use these vectors to rewrite the matrix elements using the following results,

$$
\begin{aligned}
u(\alpha p) &\cong \sqrt{\alpha} u(p), && (13)\\
(\not{p}_1 - \not{k})\not{p}_2 &= \not{\bar{r}}_1 \not{p}_2 && (14)\\
&= u_\lambda(\bar{r}_1)\bar{u}_\lambda(\bar{r}_1)\not{p}_2, && (15)\\
\not{p}_1(\not{p}_2 + \not{k}) &= \not{p}_1 u_\lambda(\bar{r}_2)\bar{u}_\lambda(\bar{r}_2), && (16)
\end{aligned}
$$

where $\cong$ denotes "equal except for an overall complex phase", and all the results rely on the assumed masslessness of $p_{1,2}$. Inserting these into the matrix elements we obtain

$$
\begin{aligned}
\mathcal{M}_3^+ &\cong g_s N\sqrt{x_2}\, \bar{u}_\lambda(r_2)\omega^\mu u_\lambda(\bar{r}_1)\bar{u}_\lambda(\bar{r}_1)\not{p}_2 u_\lambda(p_1)J_\mu(q) && (17)\\
&\equiv C^+\mathcal{M}_2(\bar{r}_1, r_2), && (18)\\
C^+ &= g_s N\sqrt{x_2}\, \bar{u}_\lambda(\bar{r}_1)\not{p}_2 u_\lambda(p_1), && (19)\\
\mathcal{M}_3^- &\equiv C^-\mathcal{M}_2(r_1, \bar{r}_2), && (20)\\
C^- &= g_s N\sqrt{x_1}\, \bar{u}_\lambda(p_2)\not{p}_1 u_\lambda(\bar{r}_2), && (21)
\end{aligned}
$$

where $\mathcal{M}_2(q_1, q_2) = \bar{u}_\lambda(q_2)\omega^\mu u_\lambda(q_1)J_\mu(q)$ is the parton-model matrix element for the current to scatter an incoming quark $q_1$, to an outgoing quark $q_2$. Finally we can calculate the $|C^\pm|^2$ explicitly to give

$$
\begin{aligned}
|C^+|^2 &= \frac{8\pi\alpha_s}{(-1-x_1)(1-x_2)Q^2}x_2^2, && (22)\\
|C^-|^2 &= \frac{8\pi\alpha_s}{(-1-x_1)(1-x_2)Q^2}x_1^2. && (23)
\end{aligned}
$$

## 2.2 Kinematics and Phase-Space

We parametrise the parton model scattering by $x_{\mathrm{B}}$, $Q^2$ and $\Phi$, the lab-frame azimuth of the lepton scattering, which is uniform for leptons with no transverse polarisation. In addition, we parametrise the hadron-plane momenta by $x_{1,2}$ and $\phi$, the azimuth of the outgoing quark around the boson-hadron axis in their cmf (or, equivalently, the Breit frame). To be precise, when discussing the specific case of DIS, $\phi = 0$ when the outgoing lepton and quark are parallel. The phase-space limits are

$$
\begin{aligned}
\frac{-1}{x_{\mathrm{B}}} &< x_1 < -1, && (24)\\
1 + x_1 &< x_2 < 1. && (25)
\end{aligned}
$$

The cross-section at $\mathcal{O}(1)$ is then

$$
\begin{aligned}
d\sigma_2 &= \frac{1}{64\pi}\,\frac{1}{s^2 x_{\rm B}^2} f(x_{\rm B},Q^2)dQ^2 dx_{\rm B}\frac{d\Phi}{2\pi}\,\Sigma|\mathcal{M}_2|^2 && (26)\\
&\equiv d\Gamma_2\Sigma|\mathcal{M}_2|^2, && (27)
\end{aligned}
$$

and at $\mathcal{O}(\alpha_s)$,

$$
\begin{aligned}
d\sigma_3 &= \frac{C_{\rm F}}{128(2\pi)^3}\,\frac{1}{s^2x_{\rm B}^2} f(-x_{\rm B}x_1,Q^2)dQ^2dx_{\rm B}\frac{d\Phi}{2\pi}\frac{dx_1}{x_1^2}dx_2\frac{d\phi}{2\pi}\,Q^2\Sigma|\mathcal{M}_3|^2 && (28)\\
&= \frac{C_{\rm F}}{4(2\pi)^2}d\Gamma_2\frac{-x_{\rm B}x_1 f(-x_{\rm B}x_1,Q^2)}{x_{\rm B}f(x_{\rm B},Q^2)}\frac{dx_1}{-x_1^3}dx_2\frac{d\phi}{2\pi}\,Q^2\Sigma|\mathcal{M}_3|^2 && (29)\\
&= \frac{C_{\rm F}\alpha_s}{2\pi}d\Gamma_2\frac{-x_{\rm B}x_1 f(-x_{\rm B}x_1,Q^2)}{x_{\rm B}f(x_{\rm B},Q^2)}\frac{dx_1dx_2}{-x_1^3(-1-x_1)(1-x_2)}\,\frac{d\phi}{2\pi}\\
&\quad\left\{x_1^2|\mathcal{M}_2(r_1,\bar{r}_2)|^2+x_2^2|\mathcal{M}_2(\bar{r}_1,r_2)|^2\right\}. && (30)
\end{aligned}
$$

It is immediately clear that this is closely related to the $e^+e^-$ formula (1), and is also an exact factorisation of the QCD and electroweak parts of the process.

However there is one important difference from the $e^+e^-$ case: while the parton-model configurations described by $r_1$ and $r_2$ are related by a rotation in $e^+e^-$, they are related by a transverse boost in the scattering process. This means that the simple Monte Carlo prescription is not possible because although it seems natural to generate lowest order $e^+e^-$ annihilation events with all possible orientations, it is not so natural to generate scattering events with all possible intrinsic transverse momenta.

It is worth noting that $x_2$ is not constrained to be positive, so the vector $r_2$ can have a negative energy-component. If one forgets this fact, and simply evaluates the resulting matrix elements, then (30) works correctly, but to provide a physical interpretation, one should first use $CPT$-invariance to rewrite the matrix element to scatter a quark from $\bar{r}_1$ to $r_2$ as the matrix element to scatter an antiquark from $-r_2$ to $-\bar{r}_1$.

In generating events, it is more convenient to introduce different phase-space variables, $x_p \equiv -1/x_1$ and $z_p \equiv \frac{p_2\cdot P}{q\cdot P} = 1+(1-x_2)/x_1$, which have independent phase-space limits

$$
\begin{aligned}
x_{\rm B} < &\; x_p < 1, && (31)\\
0 < &\; z_p < 1. && (32)
\end{aligned}
$$

Inverting the relations we get

$$
\begin{aligned}
x_1 &= -\frac{1}{x_p}, && (33)\\
x_2 &= 1-\frac{1-z_p}{x_p}. && (34)
\end{aligned}
$$

We also make use of $x_\perp$, the transverse momentum, measured in units of $Q/2$,

$$x_\perp^2 = \frac{4(1-x_p)(1-z_p)z_p}{x_p} \tag{35}$$

to rewrite the expressions for $|C^\pm|^2$,

$$|C^+|^2 = \frac{8\pi\alpha_s}{(1-x_p)(1-z_p)Q^2}\left\{x_p^2(x_2^2+x_\perp^2)\right\}\frac{x_2^2}{x_2^2+x_\perp^2}, \tag{36}$$

$$|C^-|^2 = \frac{8\pi\alpha_s}{(1-x_p)(1-z_p)Q^2}\left\{1\right\}. \tag{37}$$

The reason for writing $|C^+|^2$ in this form is that as $x_2$ tends to zero, the energy of $r_2$ tends to infinity, and the matrix element $|\mathcal{M}_2(\bar{r}_1, r_2)|^2$ in general diverges as $x_\perp^2/x_2^2$, so the product

$$\frac{x_2^2}{x_2^2+x_\perp^2}|\mathcal{M}_2(\bar{r}_1, r_2)|^2 \tag{38}$$

remains finite. The expressions in curly brackets in $|C^\pm|^2$ both lie between zero and one throughout the physical phase-space.

The cross-section is then

$$d\sigma = \frac{C_F\alpha_s}{2\pi}d\Gamma_2\frac{\frac{x_B}{x_p}f(\frac{x_B}{x_p},Q^2)}{x_B f(x_B,Q^2)}\frac{dx_p dz_p}{(1-x_p)(1-z_p)}\frac{d\phi}{2\pi}\left\{|\mathcal{M}_2(r_1,\bar{r}_2)|^2 + \left(x_p^2(x_2^2+x_\perp^2)\right)\frac{x_2^2}{x_2^2+x_\perp^2}|\mathcal{M}_2(\bar{r}_1,r_2)|^2\right\}. \tag{39}$$

The product $d\Gamma_2|\mathcal{M}_2(r_1,\bar{r}_2)|^2$ is exactly the lowest order differential cross-section, so corresponding events are provided by a parton-model event generator, but $|\mathcal{M}_2(\bar{r}_1, r_2)|^2$ requires us to reevaluate the lowest order matrix element for the new momenta.

The Monte Carlo procedure is then as follows:

1. Generate a parton model event according to the exact $\mathcal{O}(1)$ matrix element.

2. Generate $x_p$ and $z_p$ values according to $dx_p dz_p/((1-x_p)(1-z_p))$.

3. Generate a $\phi$ value uniformly, and construct the corresponding momenta $p_1$, $p_2$, $k$ and $r_{1,2}$.

4. Calculate the ratio

$$R_2 \equiv \frac{x_2^2}{x_2^2+x_\perp^2}\frac{|\mathcal{M}_2(\bar{r}_1,r_2)|^2}{|\mathcal{M}_2(r_1,\bar{r}_2)|^2}. \tag{40}$$

5. Calculate a weight factor

$$w \equiv \frac{C_{\mathrm{F}}\alpha_s}{2\pi} \frac{\frac{x_{\mathrm{B}}}{x_p} f(\frac{x_{\mathrm{B}}}{x_p}, Q^2)}{x_{\mathrm{B}} f(x_{\mathrm{B}}, Q^2)} \left\{1 + x_p^2(x_2^2 + x_\perp^2)R_2\right\}. \tag{41}$$

6. Keep the event with probability proportional to $w$.

This produces the *exact* distributions of $x_p$, $z_p$ and $\phi$, for the given lowest-order phase-space point. The average value of the weight factor is the total $\mathcal{O}(\alpha_s)$ correction to the cross-section (at tree-level, according to the chosen cutoff).

This is as far as one can take the exact calculation for a general quark scattering process, but if we now specialise to the DIS case, we can proceed further. The ratio $R_2$ can be quite generally written

$$R_2 = \frac{\cos^2\theta_2 + \mathcal{A}\cos\theta_2\left(l - \sqrt{l^2-1}\sin\theta_2\cos\phi\right) + \left(l - \sqrt{l^2-1}\sin\theta_2\cos\phi\right)^2}{1 + \mathcal{A}l + l^2}, \tag{42}$$

where $\cos\theta_2 = x_2/\sqrt{x_2^2 + x_\perp^2}$, $\sin\theta_2 = x_\perp/\sqrt{x_2^2 + x_\perp^2}$, and $l = 2/y_{\mathrm{B}} - 1$, are all Lorentz-invariant quantities that have simple interpretations in the Breit frame: $\theta_2$ is the angle between $p_2$ and the exchanged boson direction, and $Ql/2$ is the energy of the incoming lepton. $\mathcal{A}$ is related to the couplings of the fermions to the exchanged bosons,

$$\mathcal{A} = \frac{8C_{V,\ell}C_{A,\ell}C_{V,q}C_{A,q}}{(C_{V,\ell}^2 + C_{A,\ell}^2)(C_{V,q}^2 + C_{A,q}^2)}. \tag{43}$$

For pure photon exchange $\mathcal{A}_\gamma = 0$, for charged-current interactions $\mathcal{A}_{\mathrm{CC}} = 2$, and the full neutral-current case including $\gamma$-Z interference can be calculated from

$$C_{V,i} = Q_i + (I_{3,i}/2 - Q_i\sin^2\theta_w)\frac{Q^2}{(Q^2 + m_{\mathrm{Z}}^2)\sin\theta_w\cos\theta_w}, \tag{44}$$

$$C_{A,i} = I_{3,i}/2 \; \frac{Q^2}{(Q^2 + m_{\mathrm{Z}}^2)\sin\theta_w\cos\theta_w}. \tag{45}$$

Polarisation effects can also be incorporated by using appropriate couplings in $\mathcal{A}$. Using these expressions we can take the azimuthal average of $R_2$ analytically and generate the $\phi$ distribution exactly, improving the Monte Carlo weight distribution. It also allows a direct interpretation of the azimuthal effects, as we discuss in a later section.

# 3 Boson Gluon Fusion

The treatment of boson gluon fusion is mostly similar to QCD Compton, so we do not go into as great detail.

The matrix element is

$$\mathcal{M}_3(\lambda,\rho) = ig_s\bar{u}_\lambda(p_2)\left[\not\epsilon_\rho(k)\frac{-(\not p_2-\not k)}{-2\,p_2\cdot k}\omega^\mu + \omega^\mu\frac{(\not p_1-\not k)}{-2\,p_1\cdot k}\not\epsilon_\rho(k)\right]u_\lambda(p_1)J_\mu(q), \quad (46)$$

where the momenta of the quark and antiquark are $p_2$ and $p_1$, and all else is as before. This can be simply obtained from the QCD Compton case, by crossing

$$\begin{aligned} p_1 &\longrightarrow -p_1, &(47)\\ k &\longrightarrow -k. &(48)\end{aligned}$$

The special vectors are

$$\begin{aligned} r_1 &\equiv -p_1/x_1, &(49)\\ \bar{r}_2 &\equiv r_1+q = p_2-k+p_1-p_1/x_1, &(50)\\ r_2 &\equiv p_2/x_2, &(51)\\ \bar{r}_1 &\equiv r_2-q = -p_1+k-p_2+p_2/x_2. &(52)\end{aligned}$$

Note that $x_1$ now applies to the outgoing antiquark, rather than the incoming quark. This time, neither set corresponds to lowest-order scattering—both have transverse components. We obtain

$$\begin{aligned} |C^+|^2 &= \frac{8\pi\alpha_s}{(1-x_1)(1-x_2)Q^2}x_2^2, &(53)\\ |C^-|^2 &= \frac{8\pi\alpha_s}{(1-x_1)(1-x_2)Q^2}x_1^2. &(54)\end{aligned}$$

We again parametrise the kinematics by $x_p$ and $z_p$, where $z_p$ still refers to the outgoing quark, ie. particle 2, and $x_p$ refers to the incoming particle, which is this time the gluon. We then obtain

$$\begin{aligned} x_1 &= 1-\frac{z_p}{x_p}, &(55)\\ x_2 &= 1-\frac{1-z_p}{x_p}. &(56)\end{aligned}$$

This gives

$$\begin{aligned} |C^+|^2 &= \frac{8\pi\alpha_s}{z_p(1-z_p)Q^2}\left\{x_p^2(x_2^2+x_\perp^2)\right\}\frac{x_2^2}{x_2^2+x_\perp^2}, &(57)\\ |C^-|^2 &= \frac{8\pi\alpha_s}{z_p(1-z_p)Q^2}\left\{x_p^2(x_1^2+x_\perp^2)\right\}\frac{x_1^2}{x_1^2+x_\perp^2}. &(58)\end{aligned}$$

The cross-section is then

$$\begin{aligned} d\sigma = {} & \frac{\frac{1}{2}\alpha_s}{2\pi}d\Gamma_2\frac{\frac{x_{\mathrm{B}}}{x_p}f_g(\frac{x_{\mathrm{B}}}{x_p},Q^2)}{x_{\mathrm{B}}f_q(x_{\mathrm{B}},Q^2)}\frac{dx_p dz_p}{z_p(1-z_p)}\frac{d\phi}{2\pi} \\ & \left\{\left(x_p^2(x_1^2+x_\perp^2)\right)R_1 + \left(x_p^2(x_2^2+x_\perp^2)\right)R_2\right\}|\mathcal{M}_2(q_1,q_2)|^2, \qquad (59)\end{aligned}$$

where $q_{1,2}$ are the parton-model momenta, and

$$R_1 = \frac{x_1^2}{x_1^2+x_\perp^2}\,\frac{|\mathcal{M}_2(r_1,\bar{r}_2)|^2}{|\mathcal{M}_2(q_1,q_2)|^2}, \tag{60}$$

$$R_2 = \frac{x_2^2}{x_2^2+x_\perp^2}\,\frac{|\mathcal{M}_2(\bar{r}_1,r_2)|^2}{|\mathcal{M}_2(q_1,q_2)|^2}, \tag{61}$$

which can be rewritten for the explicit case of DIS as before. We obtain the identical expression for $R_2$, and the same for $R_1$, but with $\theta_2$ and $\phi$ replaced by the corresponding $\theta_1$ and $\pi-\phi$.

Up to here, the BGF cross-section has been written purely in terms of the lowest-order quark scattering (ie. not antiquarks). There is nothing wrong with this in itself, as the exact distributions of BGF events will be correctly reproduced. However, if we want to view this as a correction to the lowest-order process, rather than just a cross-section calculation, it would certainly be more desirable to treat quarks and antiquarks equivalently. We can do this by noting that the $z_p=1$ singularity is associated with configurations that become collinear to lowest-order quark scattering, while $z_p=0$ is associated with antiquark scattering. We use the separation

$$\frac{1}{z_p(1-z_p)} = \frac{1}{z_p} + \frac{1}{1-z_p} \tag{62}$$

to rewrite the cross-section

$$\begin{aligned} d\sigma &= \frac{\frac{1}{2}\alpha_s}{2\pi} d\Gamma_2 \frac{\frac{x_B}{x_p} f_g(\frac{x_B}{x_p},Q^2)}{x_B f_q(x_B,Q^2)} \frac{dx_p dz_p}{1-z_p}\frac{d\phi}{2\pi} \\ &\quad \left\{\left(x_p^2(x_1^2+x_\perp^2)\right)R_1 + \left(x_p^2(x_2^2+x_\perp^2)\right)R_2\right\}|\mathcal{M}_2(q_1,q_2)|^2 \\ &+ \frac{\frac{1}{2}\alpha_s}{2\pi} d\Gamma_2 \frac{\frac{x_B}{x_p} f_g(\frac{x_B}{x_p},Q^2)}{x_B f_q(x_B,Q^2)} \frac{dx_p dz_p}{z_p}\frac{d\phi}{2\pi} \\ &\quad \left\{\left(x_p^2(x_1^2+x_\perp^2)\right)R_1 + \left(x_p^2(x_2^2+x_\perp^2)\right)R_2\right\}|\mathcal{M}_2(q_1,q_2)|^2. \end{aligned} \tag{63}$$

Now we define a set of exchanged variables,

$$\tilde{p}_1 \equiv p_2, \tag{64}$$

$$\tilde{p}_2 \equiv p_1, \tag{65}$$

$$\tilde{z}_p \equiv 1-z_p. \tag{66}$$

Although the special vectors are defined in the same way, they become negated, because of the minus sign in (49), so we obtain

$$\begin{aligned} d\sigma &= \frac{\frac{1}{2}\alpha_s}{2\pi} d\Gamma_2 \frac{\frac{x_B}{x_p} f_g(\frac{x_B}{x_p},Q^2)}{x_B f_q(x_B,Q^2)} \frac{dx_p dz_p}{1-z_p}\frac{d\phi}{2\pi} \\ &\quad \left\{\left(x_p^2(x_1^2+x_\perp^2)\right)R_1 + \left(x_p^2(x_2^2+x_\perp^2)\right)R_2\right\}|\mathcal{M}_2(q_1,q_2)|^2 \end{aligned}$$

$$
\begin{aligned}
&+ \quad \frac{\frac{1}{2}\alpha_s}{2\pi} d\Gamma_2 \frac{\frac{x_{\rm B}}{x_p} f_g(\frac{x_{\rm B}}{x_p}, Q^2)}{x_{\rm B} f_q(x_{\rm B}, Q^2)} \frac{dx_p d\tilde{z}_p}{1-\tilde{z}_p} \frac{d\tilde{\phi}}{2\pi} \\
&\quad \left\{ \left( x_p^2(\tilde{x}_2^2 + x_\perp^2) \right) \frac{\tilde{x}_2^2}{\tilde{x}_2^2 + x_\perp^2} |\mathcal{M}_2(-\tilde{r}_2, -\tilde{\bar{r}}_1)|^2 \right. \\
&\quad \left. + \left( x_p^2(\tilde{x}_1^2 + x_\perp^2) \right) \frac{\tilde{x}_1^2}{\tilde{x}_1^2 + x_\perp^2} |\mathcal{M}_2(-\tilde{\bar{r}}_2, -\tilde{r}_1)|^2 \right\}. \qquad (67)
\end{aligned}
$$

Finally, we can use the $CPT$-invariance of the matrix element, to write

$$
|\mathcal{M}_2(-q_2, -q_1)|^2 = |\widetilde{\mathcal{M}}_2(q_1, q_2)|^2, \qquad (68)
$$

where $\widetilde{\mathcal{M}}_2(q_1, q_2)$ is the matrix element to scatter an antiquark from $q_1$ to $q_2$. Thus the two halves of the cross-section are identical, but with quarks and antiquarks interchanged,

$$
\begin{aligned}
d\sigma \quad &= \quad \frac{\frac{1}{2}\alpha_s}{2\pi} d\Gamma_2 \frac{\frac{x_{\rm B}}{x_p} f_g(\frac{x_{\rm B}}{x_p}, Q^2)}{x_{\rm B} f_q(x_{\rm B}, Q^2)} \frac{dx_p dz_p}{1-z_p} \frac{d\phi}{2\pi} \\
&\quad \left\{ \left( x_p^2(x_1^2 + x_\perp^2) \right) R_1 + \left( x_p^2(x_2^2 + x_\perp^2) \right) R_2 \right\} |\mathcal{M}_2(q_1, q_2)|^2 \\
&+ \quad \frac{\frac{1}{2}\alpha_s}{2\pi} d\Gamma_2 \frac{\frac{x_{\rm B}}{x_p} f_g(\frac{x_{\rm B}}{x_p}, Q^2)}{x_{\rm B} f_{\bar{q}}(x_{\rm B}, Q^2)} \frac{dx_p d\tilde{z}_p}{1-\tilde{z}_p} \frac{d\tilde{\phi}}{2\pi} \\
&\quad \left\{ \left( x_p^2(\tilde{x}_1^2 + x_\perp^2) \right) \tilde{R}_1 + \left( x_p^2(\tilde{x}_2^2 + x_\perp^2) \right) \tilde{R}_2 \right\} |\widetilde{\mathcal{M}}_2(q_1, q_2)|^2. \qquad (69)
\end{aligned}
$$

The two halves can then be separately associated with lowest-order scattering of quarks and antiquarks.

The Monte Carlo algorithm is then:

1. Generate a parton model quark or antiquark event according to the exact $\mathcal{O}(1)$ matrix element.
2. Generate $x_p$ and $z_p$ values according to $dx_p dz_p/(1-z_p)$.
3. Generate a $\phi$ value uniformly, and construct the corresponding momenta $p_1$, $p_2$, $k$ and $r_{1,2}$.
4. Calculate the ratios $R_1$ and $R_2$.
5. Calculate a weight factor

$$
w = \frac{\frac{1}{2}\alpha_s}{2\pi} \frac{\frac{x_{\rm B}}{x_p} f_g(\frac{x_{\rm B}}{x_p}, Q^2)}{x_{\rm B} f_{q/\bar{q}}(x_{\rm B}, Q^2)} \left\{ x_p^2(x_1^2 + x_\perp^2) R_1 + x_p^2(x_2^2 + x_\perp^2) R_2 \right\}. \qquad (70)
$$

6. Keep the event with probability proportional to $w$.

This again produces the *exact* distributions at the given phase-space point, and gives the total tree-level $\mathcal{O}(\alpha_s)$ correction there.

# 4 Lepton-Hadron Correlations in DIS

Before discussing the azimuthal correlations that arise in first order QCD, it is worth recalling that a correlation also arises in the parton model, if the parton's intrinsic $p_t$ in a hadron is included. This is because at fixed $Q^2$, different azimuths correspond to different parton-lepton collision energies, so even though the Fermi motion of partons in a hadron is azimuthally uniform, their scattering cross-section is not. The matrix element is identical to $|\mathcal{M}_2(\bar{r}_1, r_2)|^2$ evaluated earlier,

$$|\mathcal{M}|^2 \propto \frac{\cos^2\theta_2 + \mathcal{A}\cos\theta_2\left(l - \sqrt{l^2-1}\sin\theta_2\cos\phi\right) + \left(l - \sqrt{l^2-1}\sin\theta_2\cos\phi\right)^2}{1+\mathcal{A}l+l^2}. \tag{71}$$

It is this partonic matrix element that determines the azimuthal asymmetry[5], and not the corresponding partonic cross-section ($\sim |\mathcal{M}|^2/s$, where $s$ is the parton-lepton invariant mass). $\theta_2$ can be directly calculated since in the Breit frame, the incoming parton has longitudinal momentum $Q/2$ and transverse momentum $p_t$, so we have

$$\tan\theta_2 = 2p_t/Q. \tag{72}$$

The size of the correlation is usually parametrised by the average values of $\cos\phi$ and $\cos 2\phi$,

$$\begin{aligned}
\langle\cos\phi\rangle &= \frac{-\mathcal{A}\cos\theta_2\sqrt{l^2-1}\sin\theta_2 - 2l\sqrt{l^2-1}\sin\theta_2}{2(\cos^2\theta_2 + \mathcal{A}\cos\theta_2 l + l^2 + \frac{1}{2}(l^2-1)\sin^2\theta_2)}, &(73)\\
\langle\cos 2\phi\rangle &= \frac{\frac{1}{2}(l^2-1)\sin^2\theta_2}{2(\cos^2\theta_2 + \mathcal{A}\cos\theta_2 l + l^2 + \frac{1}{2}(l^2-1)\sin^2\theta_2)}. &(74)
\end{aligned}$$

It can be seen that both effects are maximised by working at small $Q^2$, so that $\theta_2$ is maximised (though it is still small for accessible values of $Q^2$). It is also increased somewhat by working at small $y_{\rm B}$ (ie. $l \gg 1$). Taking the limit $p_t \ll Q$ and using the definition of $l$, we obtain the usual expressions[5],

$$\begin{aligned}
\langle\cos\phi\rangle &= \frac{(2-y_{\rm B}+\frac{1}{2}\mathcal{A}y_{\rm B})\sqrt{1-y_{\rm B}}}{1+(1-y_{\rm B})^2+\frac{1}{2}\mathcal{A}y_{\rm B}(2-y_{\rm B})}\left(\frac{-2p_t}{Q}\right), &(75)\\
\langle\cos 2\phi\rangle &= \frac{2(1-y_{\rm B})}{1+(1-y_{\rm B})^2+\frac{1}{2}\mathcal{A}y_{\rm B}(2-y_{\rm B})}\left(\frac{p_t^2}{Q^2}\right). &(76)
\end{aligned}$$

In the small-$y_{\rm B}$ limit, these cross-sections become independent of $\mathcal{A}$ and, as noted in [5] are even the same if the fermions are replaced by scalars. This corresponds to the well-known fact that the cross-section for scattering by exchange of a single spin-1 particle has the same high-energy behaviour,

$$|\mathcal{M}|^2 \propto \left(\frac{s}{Q^2}\right)^2, \tag{77}$$

independent of its vector/axial-vector nature, its couplings, and the particles being scattered. This is the dominant contribution, even when $y_{\mathrm{B}}$ is not small.

Turning now to QCDC, we recall that the total cross-section is the weighted sum of parton-model pieces where there is no $p_t$, and where there is a $p_t$ of

$$p_t^2 = \tfrac{1}{4}Q^2\frac{x_\perp^2}{x_2^2} = Q^2\frac{(1-x_p)(1-z_p)x_pz_p}{(x_p+z_p-1)^2}, \tag{78}$$

whose relative importance is reduced by $Q^2/(Q^2+4p_t^2)$.

Studying the first-order cross-section (30), it is clear that only $|\mathcal{M}_2(\bar{r}_1,r_2)|^2$ generates any $\phi$-dependence, and that this is identical to that in the parton model with intrinsic $p_t$ given by (78). One can therefore say that QCD does not play a *direct* part in determining the azimuthal correlations. Its rôle can be summarised as providing a large 'intrinsic' $p_t$, and then diluting the resulting correlation. Furthermore, as mentioned above, this is dominated by the fact that the exchanged particle has spin-1. This also applies to the BGF part, although the dilution is not so great, because both contributions have an 'intrinsic' $p_t$.

We can calculate the size of the correlation,

$$\langle\cos\phi\rangle = \frac{\int d\sigma_3 \cos\phi}{\int d\sigma_3}, \tag{79}$$

$$\langle\cos 2\phi\rangle = \frac{\int d\sigma_3 \cos 2\phi}{\int d\sigma_3}, \tag{80}$$

where the integrals are over whatever phase-space region is selected for the analysis. We examine two regions in particular, firstly the point where the correlation is maximised. Studying (39), we find that both $\langle\cos\phi\rangle$ and $\langle\cos 2\phi\rangle$ are maximised at $x_p = z_p = 1/2$. This corresponds to scattering in which both outgoing partons are at 90° to the boson-hadron axis in the Breit frame, with energy $Q/2$, so $\sqrt{\hat{s}} = 2p_t = Q$. Going to higher $p_t$ increases the size of the correlation generated by $|\mathcal{M}_2(\bar{r}_1,r_2)|^2$, but also increases the dilution, so that the correlation gets smaller overall. At that point we have

$$\langle\cos\phi\rangle_{\mathrm{QCDC,max}} = \frac{-2\sqrt{1-y_{\mathrm{B}}}(2-y_{\mathrm{B}})}{9(1+(1-y_{\mathrm{B}})^2)+4(1-y_{\mathrm{B}})+4\mathcal{A}y_{\mathrm{B}}(2-y_{\mathrm{B}})}, \tag{81}$$

$$\langle\cos 2\phi\rangle_{\mathrm{QCDC,max}} = \frac{\frac{1}{4}(2-y_{\mathrm{B}})^2}{9(1+(1-y_{\mathrm{B}})^2)+4(1-y_{\mathrm{B}})+4\mathcal{A}y_{\mathrm{B}}(2-y_{\mathrm{B}})}. \tag{82}$$

The BGF case is not quite so simple, because although the contributions to $\langle\cos\phi\rangle$ from the $R_1$ and $R_2$ terms in (69) are separately maximised at $x_p = z_p = 1/2$, they are equal and opposite there, so exactly cancel. The sum is maximised at $x_p = z_p = (2+\sqrt{8\sqrt{3}-12})/4 \approx 0.841$, which corresponds to a configuration where one of the partons is at 90° to the boson-hadron axis, and the other is about 20° from the current direction, with $p_t \approx 0.159Q$ and $\sqrt{\hat{s}} \approx 0.435Q$. The value at that point does not have a simple form, but is numerically similar to $\langle\cos\phi\rangle_{\rm QCDC,max}$. It would not be as easy to measure though, since different parts of phase-space give correlations with different signs, so integrating over some region of phase-space reduces $\langle\cos\phi\rangle$ faster for BGF than for QCDC. For $\langle\cos 2\phi\rangle$, the maximum is again at $x_p = z_p = 1/2$, with value

$$\langle\cos 2\phi\rangle_{\rm BGF,max} = \frac{1-y_{\rm B}}{1+(1-y_{\rm B})^2+4(1-y_{\rm B})}, \tag{83}$$

independent of $\mathcal{A}$, almost four times larger than $\langle\cos 2\phi\rangle_{\rm QCDC,max}$, and comparable to $\langle\cos\phi\rangle_{\rm QCDC,max}$.

As already mentioned, as the transverse momentum is increased above $Q/2$, the correlation becomes weaker again. This is because the correlation generated by $|\mathcal{M}_2(\bar{r}_1, r_2)|^2$ is governed by the direction of $p_2$ in the Breit frame, rather than its $p_t$. Thus the correlation cannot get any stronger than it is when $p_2$ is at 90° to the current direction. However, the dilution by the azimuthally flat term increases with increasing $\hat{s}$, so the correlation decreases overall. Since most experimental analyses use a fixed cutoff in $p_t$ irrespective of $Q$, it is primarily this dependence that determines the strong overall dependence on $Q^2$.

The other phase-space we consider is to not make any cuts at all. This is possible because both $\langle\cos\phi\rangle$ and $\langle\cos 2\phi\rangle$ are infrared safe quantities, so if $\phi$ is measured semi-inclusively for all DIS events, the expectation values can be expanded as simple power series in $\alpha_s$[‡]. We can then write the expectations symbolically as

$$\langle\cos\phi\rangle = \frac{\int d\sigma_3 \cos\phi}{1+\int d\sigma_3 - C\alpha_s}, \tag{84}$$

with an equivalent expression for $\langle\cos 2\phi\rangle$. Because the integrals are now over the whole phase-space, the integral in the denominator is divergent, but $C$, the first-order virtual correction to the lowest-order result, is also divergent such that after renormalisation and factorisation their sum is the finite first-order QCD correction to the total DIS cross-section. The integral in the numerator is convergent. Since it is first-order in $\alpha_s$, we can ignore the $\alpha_s$ dependence of the denominator to first order, and we obtain simply

$$\langle\cos\phi\rangle = \int d\sigma_3 \cos\phi. \tag{85}$$

[‡]This is only strictly true if we define $\phi$ in such a way that the expectation values are identical in the $p_t \to 0$ limit and at $p_t = 0$, ie. if they are zero in the latter case. This can be achieved by adding the rule that if no particles in the event have any momentum transverse to the boson-hadron axis, a $\phi$ value is chosen randomly and uniformly. Since experimentally such events never exist, this makes no practical difference to the result.

For QCDC we obtain

$$\begin{aligned}\langle\cos\phi\rangle_{\mathrm{QCDC}} &= -\frac{C_{\mathrm{F}}\alpha_s}{4\pi}\int_{x_{\mathrm{B}}}^1 dx_p\int_0^1 dz_p\frac{1}{(1-x_p)(1-z_p)}\frac{\frac{x_{\mathrm{B}}}{x_p}f(\frac{x_{\mathrm{B}}}{x_p},Q^2)}{x_{\mathrm{B}}f(x_{\mathrm{B}},Q^2)}\\ & \qquad x_p^2(x_2^2+x_\perp^2)\frac{\mathcal{A}\sqrt{l^2-1}\cos\theta_2\sin\theta_2+2l\sqrt{l^2-1}\sin\theta_2}{1+\mathcal{A}l+l^2},\end{aligned}\tag{86}$$

which can be integrated over $z_p$ to give

$$\begin{aligned}\langle\cos\phi\rangle_{\mathrm{QCDC}} &= -\frac{C_{\mathrm{F}}\alpha_s}{16}\int_{x_{\mathrm{B}}}^1 dx_p\sqrt{\frac{x_p}{1-x_p}}\frac{\frac{x_{\mathrm{B}}}{x_p}f(\frac{x_{\mathrm{B}}}{x_p},Q^2)}{x_{\mathrm{B}}f(x_{\mathrm{B}},Q^2)}\\ & \qquad \frac{\mathcal{A}\sqrt{l^2-1}(4x_p-1)+2l\sqrt{l^2-1}(1+2x_p)}{1+\mathcal{A}l+l^2},\end{aligned}\tag{87}$$

which must be integrated numerically. We similarly obtain

$$\langle\cos 2\phi\rangle_{\mathrm{QCDC}} = \frac{C_{\mathrm{F}}\alpha_s}{4\pi}\frac{l^2-1}{1+\mathcal{A}l+l^2}\int_{x_{\mathrm{B}}}^1 dx_p x_p\frac{\frac{x_{\mathrm{B}}}{x_p}f(\frac{x_{\mathrm{B}}}{x_p},Q^2)}{x_{\mathrm{B}}f(x_{\mathrm{B}},Q^2)},\tag{88}$$

and

$$\begin{aligned}\langle\cos\phi\rangle_{\mathrm{BGF}} &= -\frac{\frac{1}{2}\alpha_s}{8}\int_{x_{\mathrm{B}}}^1 dx_p\sqrt{x_p(1-x_p)}\frac{\frac{x_{\mathrm{B}}}{x_p}f_g(\frac{x_{\mathrm{B}}}{x_p},Q^2)}{x_{\mathrm{B}}f_q(x_{\mathrm{B}},Q^2)}\\ & \qquad \frac{\mathcal{A}\sqrt{l^2-1}+2l\sqrt{l^2-1}(2x_p-1)}{1+\mathcal{A}l+l^2},\end{aligned}\tag{89}$$

$$\langle\cos 2\phi\rangle_{\mathrm{BGF}} = \frac{\frac{1}{2}\alpha_s}{2\pi}\frac{l^2-1}{1+\mathcal{A}l+l^2}\int_{x_{\mathrm{B}}}^1 dx_p x_p(1-x_p)\frac{\frac{x_{\mathrm{B}}}{x_p}f_g(\frac{x_{\mathrm{B}}}{x_p},Q^2)}{x_{\mathrm{B}}f_q(x_{\mathrm{B}},Q^2)}.\tag{90}$$

Note that these are the extreme values of the expectations, assuming that the scattered parton direction could be perfectly identified. They would be reduced by a realistic method, such as using the hadron with largest Feynman-$x_{\mathrm{F}}$, or using all particles weighted by $x_{\mathrm{F}}$. The values of these expectations are shown in Fig. 2, in comparison with those from the intrinsic $p_t$ in the parton model.

Although we have seen that the physical origin of the correlation is the same in QCD as in the parton model, the dependence on $x_{\mathrm{B}}$ and $Q^2$ is quite difference, so the two contributions can be easily separated.

# 5 The Drell-Yan Process

The treatment of the Drell-Yan process again proceeds along similar lines. We start with the annihilation+gluon process, $\mathrm{q\bar{q}}\to\mathrm{gV}^*$, for which the matrix element is

$$\mathcal{M}_3(\lambda,\rho) = ig_s\bar{v}_\lambda(p_2)\left[\not\epsilon_\rho(k)\frac{(\not p_2-\not k)}{-2\,p_2\!\cdot\!k}\omega^\mu+\omega^\mu\frac{-(\not p_1-\not k)}{-2\,p_1\!\cdot\!k}\not\epsilon_\rho(k)\right]u_\lambda(p_1)J_\mu(q),\tag{91}$$

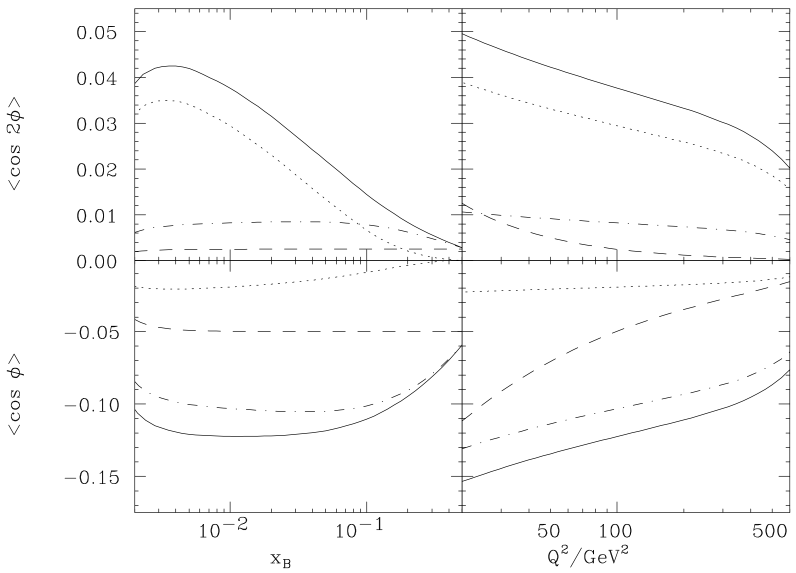


Figure 2: The average values of $\cos\phi$ and $\cos 2\phi$ from the parton model (dashed) and QCD (solid), for ep collisions at $s = 10^5\,\mathrm{GeV}^2$ with $Q^2 = 10^2\,\mathrm{GeV}^2$ (left) and $x_{\mathrm{B}} = 0.01$ (right). We use the MRS D−′ distribution functions, $\Lambda_{\mathrm{QCD}} = 230\,\mathrm{MeV}$, with pure photon exchange, and $\langle p_t\rangle = \sqrt{\langle p_t^2\rangle} = 500\,\mathrm{MeV}$. The QCD curves are also broken down into the separate contributions from QCDC (dot-dashed) and BGF (dotted).

where the momenta of the quark and antiquark are $p_1$ and $p_2$. This can again be obtained from the QCD Compton case, by crossing

$$p_2 \longrightarrow -p_2. \tag{92}$$

The special vectors are

$$\begin{aligned} r_1 &\equiv p_1/x_1, & (93)\\ \bar{r}_2 &\equiv q - r_1 = p_2 - k + p_1 - p_1/x_1, & (94)\\ r_2 &\equiv p_2/x_2, & (95)\\ \bar{r}_1 &\equiv q - r_2 = p_1 - k + p_2 - p_2/x_2. & (96)\end{aligned}$$

We then obtain

$$\begin{aligned} |C^+|^2 &= \frac{8\pi\alpha_s}{(x_1-1)(x_2-1)Q^2}x_2^2, & (97)\\ |C^-|^2 &= \frac{8\pi\alpha_s}{(x_1-1)(x_2-1)Q^2}x_1^2. & (98)\end{aligned}$$

The cross-section in lowest order is

$$d\sigma_2 = \frac{1}{s}dQ^2dy\ f_{q/1}(\eta_1)f_{\bar{q}/2}(\eta_2)\frac{1}{2Q^2}|\mathcal{M}_2|^2d\Gamma_2, \tag{99}$$

where $y$ is the rapidity of the gauge boson, $\eta_{1,2} = Q/\sqrt{s}e^{\pm y}$ are the energy-fractions of the quarks in the hadrons, $f_{q/h}$ are the corresponding distribution functions, and $d\Gamma_2$ is an element of the phase-space for the gauge boson decay. The corresponding first-order cross-section is

$$\begin{aligned} d\sigma_3 &= \frac{1}{s}d\hat{s}dy\ f_{q/1}(\xi_1)f_{\bar{q}/2}(\xi_2)\frac{1}{2Q^2}\ \frac{C_F\alpha_s}{2\pi}\ \frac{dx_1dx_2}{(x_1+x_2-1)^3(x_1-1)(x_2-1)}\ \frac{d\phi}{2\pi} \\ & \left\{x_1^2|\mathcal{M}_2(r_1,\bar{r}_2)|^2 + x_2^2|\mathcal{M}_2(\bar{r}_1,r_2)|^2\right\}d\Gamma_2. \end{aligned} \tag{100}$$

Just as in the $e^+e^-$ case, this can be evaluated exactly, without any knowledge of $|\mathcal{M}_2|^2$. The event can be boosted from the lab frame to the rest frame of the boson in such a way that the azimuth of the gluon around either $p_1$ or $p_2$ is identical to its lab-frame azimuth around the beam direction. However, these two different possibilities correspond to different configurations of the boson decay in the lab frame. $|\mathcal{M}_2(r_1,\bar{r}_2)|^2$ clearly has no dependence on the azimuth around $p_1$, and $|\mathcal{M}_2(\bar{r}_1,r_2)|^2$ has no dependence on the azimuth around $p_2$. This means that the boson decays can be correctly generated by generating a uniform azimuth around one or other of the quarks in the boson's rest frame, just as in $e^+e^-$ annihilation.

It then only remains to relate the two cross-sections. Switching to using $Q^2$ and $\hat{t} = -2\,p_1\!\cdot\!k = -Q^2(x_2-1)$ to parametrise the hadron-plane momenta, we obtain

$$\begin{aligned} d\sigma_3 &= \frac{1}{s}d\hat{s}dydQ^2d\hat{t}\ f_{q/1}(\xi_1)f_{\bar{q}/2}(\xi_2)\ \frac{1}{2Q^2}\ \frac{C_F\alpha_s}{2\pi}\ \frac{1}{\hat{s}^2\hat{t}\hat{u}}\ \frac{d\phi}{2\pi} \\ & \left\{(Q^2-\hat{u})^2|\mathcal{M}_2(r_1,\bar{r}_2)|^2 + (Q^2-\hat{t})^2|\mathcal{M}_2(\bar{r}_1,r_2)|^2\right\}d\Gamma_2 \end{aligned} \tag{101}$$

and hence

$$d\sigma_3 = \frac{f_{q/1}(\xi_1)f_{\bar{q}/2}(\xi_2)}{f_{q/1}(\eta_1)f_{\bar{q}/2}(\eta_2)}\frac{C_F\alpha_s}{2\pi}\ \frac{d\hat{s}d\hat{t}}{\hat{s}^2\hat{t}\hat{u}}\left\{(Q^2-\hat{u})^2d\sigma_2\frac{d\phi}{2\pi} + (Q^2-\hat{t})^2d\sigma_2\frac{d\phi}{2\pi}\right\}. \tag{102}$$

The Monte Carlo algorithm is then

1. Generate a parton model event according to the exact $\mathcal{O}(1)$ matrix element.
2. Generate $\hat{s}$ and $\hat{t}$ values according to $Q^4d\hat{s}d\hat{t}/\hat{s}^2\hat{t}\hat{u} = Q^4d\hat{s}d\hat{t}/\hat{s}^2\hat{t}(Q^2-\hat{s}-\hat{t})$.
3. Construct momenta in the boson rest-frame corresponding to these values.
4. Choose parton 1 with probability $(Q^2-\hat{u})^2/\left((Q^2-\hat{u})^2+(Q^2-\hat{t})^2\right)$, and otherwise parton 2, and uniformly rotate about the chosen parton.
5. Boost the momenta back to the lab frame such that the boson's rapidity is the same as it was in the parton-model event.

6. Calculate a weight factor

$$w=\frac{C_{\mathrm{F}}\alpha_s}{2\pi}\frac{f_{q/1}(\xi_1)f_{\bar{q}/2}(\xi_2)}{f_{q/1}(\eta_1)f_{\bar{q}/2}(\eta_2)}\left\{(1-\hat{u}/Q^2)^2+(1-\hat{t}/Q^2)^2\right\}. \tag{103}$$

7. Keep the event with probability proportional to $w$.

This correctly gives the properties of annihilation+gluon events, for example correlations between the gluon and lepton directions, with no knowledge of the matrix element that determines them, provided a generator of lowest-order events is available.

Turning to the Compton process, qg $\to$ qV$^*$, we find that exactly the same treatment holds, and we obtain

$$d\sigma_3=\frac{f_{q/1}(\xi_1)f_{g/2}(\xi_2)}{f_{q/1}(\eta_1)f_{\bar{q}/2}(\eta_2)}\frac{\frac{1}{2}\alpha_s}{2\pi}\frac{d\hat{s}d\hat{t}}{-\hat{s}^3\hat{t}}\left\{(Q^2-\hat{t})^2d\sigma_2\frac{d\phi}{2\pi}+(Q^2-\hat{s})^2d\sigma_2\frac{d\phi}{2\pi}\right\}, \tag{104}$$

where $\hat{t}$ is this time $-2p_2{\cdot}k$. Equivalent formulæ hold when the quark is replaced by an antiquark, or comes from the other hadron.

The Monte Carlo algorithm is then

1. Generate a parton model event according to the exact $\mathcal{O}(1)$ matrix element.
2. Generate $\hat{s}$ and $\hat{t}$ values according to $-Q^4d\hat{s}d\hat{t}/\hat{s}^3\hat{t}$.
3. Construct momenta in the boson rest-frame corresponding to these values.
4. Choose parton 1 with probability $(Q^2-\hat{t})^2/\left((Q^2-\hat{t})^2+(Q^2-\hat{s})^2\right)$, and otherwise parton 2, and uniformly rotate about the chosen parton.
5. Boost the momenta back to the lab frame such that the boson's rapidity is the same as it was in the parton-model event.
6. Calculate a weight factor

$$w=\frac{\frac{1}{2}\alpha_s}{2\pi}\frac{f_{q/1}(\xi_1)f_{g/2}(\xi_2)}{f_{q/1}(\eta_1)f_{\bar{q}/2}(\eta_2)}\left\{(1-\hat{t}/Q^2)^2+(1-\hat{s}/Q^2)^2\right\}. \tag{105}$$

7. Keep the event with probability proportional to $w$.

This again gives the correct event properties, with no knowledge of the matrix element that determines them, provided a generator of lowest-order events is available.

# 6 Summary

By working in the simple gauge introduced by the CALKUL collaboration, it is possible to *exactly* factorise the first order corrections to the electroweak production, scattering and annihilation of quarks. This allows a transparent understanding of event properties and correlations, and enables simple Monte Carlo prescriptions to be constructed. This was done in [1] for production processes, and in the present paper for scattering and annihilation processes.

For production and annihilation the factorisation is complete, in the sense that the Monte Carlo algorithm does not need any details of the lowest-order cross-section to generate the correction. This is because it is able to use the angular configurations generated at lowest order, provided that all such configurations are generated. In the scattering case, the equivalent requirement is that all transverse boosts are generated, which is not a natural situation. Instead, the lowest order matrix element must be reevaluated for a new set of momenta.

As an example of the additional insight that our approach can give, we discussed azimuthal correlations between the leptonic and hadronic planes in DIS. It was seen that the correlation that arises in first-order QCD has the same physical origin as that in the parton model—simply the variation of the parton-lepton invariant mass with azimuth, when there is a non-zero transverse momentum. The rôle of QCD is simply to provide that transverse momentum. By separating the cross-section into two components, our method is able to describe this transverse momentum in a gauge-invariant way.

We finally note that since our results for first-order cross-sections are explicitly formulated as corrections to lowest-order cross-sections, they are ideally suited for making first-order matrix-element corrections to parton shower algorithms[6].

# References


1. R. Kleiss, Phys. Lett. 180B (1986) 400.

2. H. Georgi, H.D. Politzer, Phys. Rev. Lett. 40 (1978) 3.

3. J. Chay, S.D. Ellis, W.J. Stirling, Phys. Rev. D45 (1992) 46.

4. The CALKUL Collaboration, Nucl. Phys. B206 (1982) 53.

5. R.N. Cahn, Phys. Lett. 78B (1978) 269.
   R.N. Cahn, Phys. Rev. D40 (1989) 3107.

6. M.H. Seymour, LU TP 94-12, contributed to the 27th International Conference on High Energy Physics, Glasgow, U.K., 20–27 July 1994.
   M.H. Seymour, *Matrix-Element Corrections to Angular-Ordered Parton Showers,* in preparation.